



ACCURACY EVALUATION

GEOREFERENCING HOVERMAP POINT CLOUDS USING
'BEST-FIT' SPHERE REGISTRATION IN CLOUDCOMPARE

Dr. Jeremy J. Sofonia, CEnvP - Solution Manager, Emesent

GEOREFERENCING HOVERMAP POINT CLOUDS USING ‘BEST-FIT’ SPHERE REGISTRATION IN CLOUDCOMPARE

INTRODUCTION

Lightweight and easy to deploy, the Emesent Hovermap LiDAR scanning system is opening new opportunities to quickly obtain high-resolution 3D data across a wide variety of applications. The versatility of Hovermap is a key feature in this and includes aerial (‘drone’), vehicle and walking capabilities to name a few.

Understanding performance strengths, and limitations, of any scanning system is critical to achieving project goals regardless of how it is deployed. In many scenarios, this is achieved through a comparison of the point cloud(s) obtained to accurate ‘known’ control points. The use of laser scanning spheres for this purpose is well established across the industry as they facilitate accurate georeferencing, co-registration of multiple scans and can provide valuable baseline for quality assurance. Here, we examine the accuracy of Hovermap at a working quarry through the deployment of laser scanning spheres as control points and a ‘best-fit’ registration method using the CloudCompare software package.

Results from this show that the Hovermap data fits the survey control with an RMSE of 14mm and a mean pair-wise 3D distance measure of 13mm ± 4mm from ground truth.

METHODS

CONTROL AND DATA CAPTURE

Upon arriving to site, four control points were established across the study area by a licensed surveyor and tripod-mounted prisms. To better visualize the control points within the point clouds during Hovermap data collection, each prism was replaced with a 0.150m Ø polystyrene spherical target. These spherical targets were designed with a fixed vertical offset that coincided with the prism position (Figure 1).

Following the establishment of control, three scans were performed using the Emesent Hovermap LiDAR system. This included two separate flights over the target area with Hovermap mounted to a DJI M210 (‘drone’) and one walking scan within and around a crushing plant (Figure 2). Point clouds of the three scans were created and merged into a unified model using the Emesent software (Figure 3) and opened in CloudCompare.



Figure 1 Establishment of control across the study area using four prisms that were (a) located with a total station. Prisms were replaced with (b) spherical targets with the same vertical offsets during the Hovermap scanning.



Figure 2 Hovermap as mounted to the DJI M210 deployed across the study area in (a, b) two flights and a walking scan of a crushing plant.

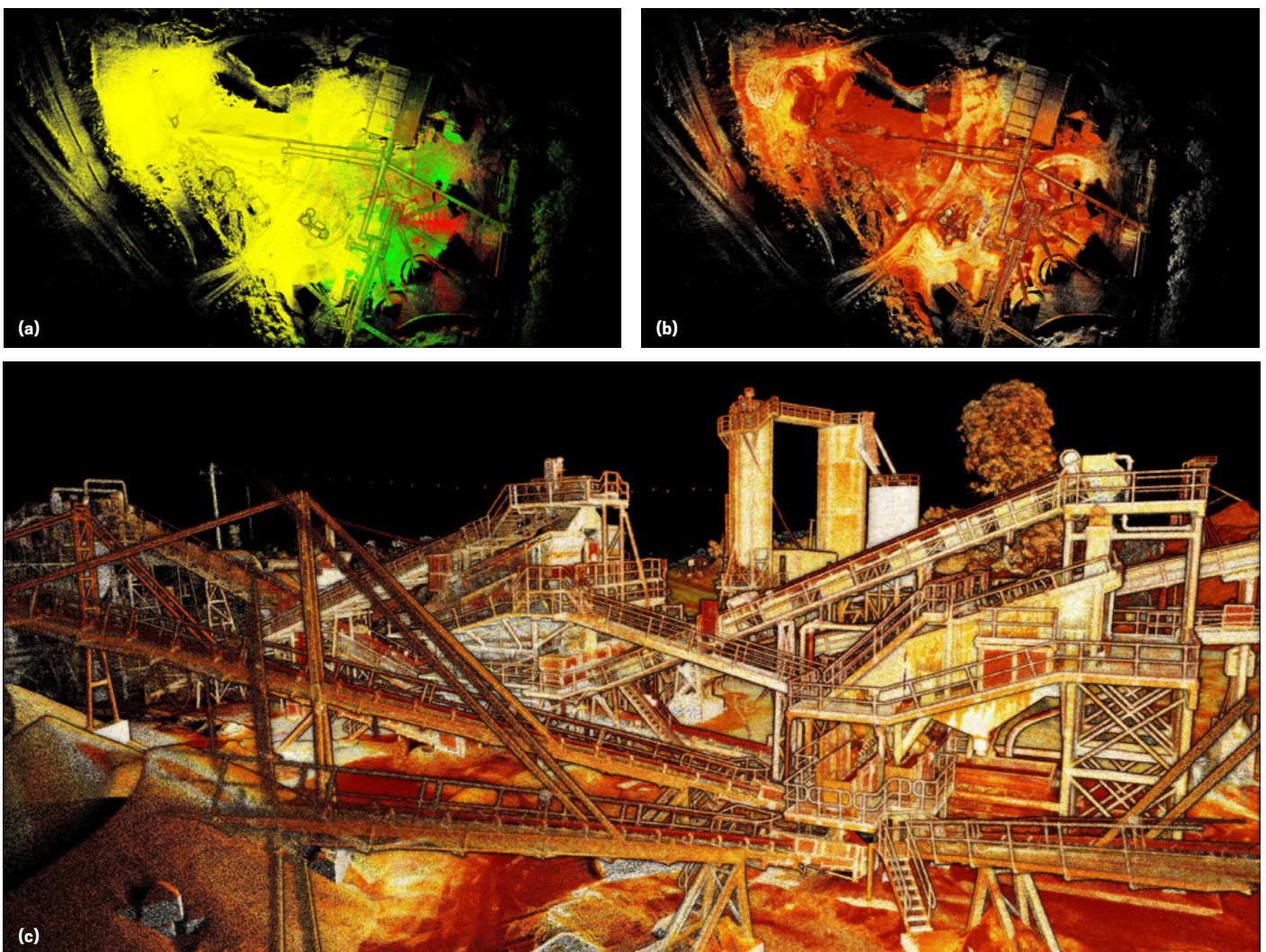


Figure 3 The (a) three point clouds obtained by Hovermap flight and walking scans, colored red, green, and yellow, aligned and merged into a unified model with the Emesent processing software. The merged point clouds, colored by intensity, shown in (b) plan and (c) perspective views.

POINT CLOUD CLEANING

Cleaning, an important part of post-processing, removes noise and thereby improves registration, visualization, subsequent measures and models as well as reduces the file size. Here, we used several tools in CloudCompare to filter the point cloud, as detailed in **Table 1.**, minimizing noise whilst retaining sufficient resolution on the target spheres to facilitate ‘best-fit’ modelling.

Table 1 Settings used to in CloudCompare, by attribute/function, to clean the point cloud prior to registration

Attribute / Function	Settings Applied
Range	1.500m (min) to 35m (max) – to remove range noise
Time	As needed to remove points collected during take-off and landing of the drone
Intensity	1 (min) to 255 (max) – to remove low intensity noise
Subsample	0.001m – Minimum distance between points – to remove duplicate points
Statistical Outlier Removal (SOR)	Mean distance estimation = 8 Standard Deviation = 2.00
Segment (Scissors) Tool	To remove ghosting of moving people through the scan area

‘BEST-FIT’ SPHERES

The creation of ‘best-fit’ spheres in CloudCompare is straightforward and was accomplished here using the Segment tool (Edit / Segment) to isolate the target sphere from the point cloud (**Figure 4**). Once isolated, the points associated with the sphere were selected within the DB Tree window and the virtual spheres created using the Fit / Sphere function under the tools menu (**Figure 4d**).

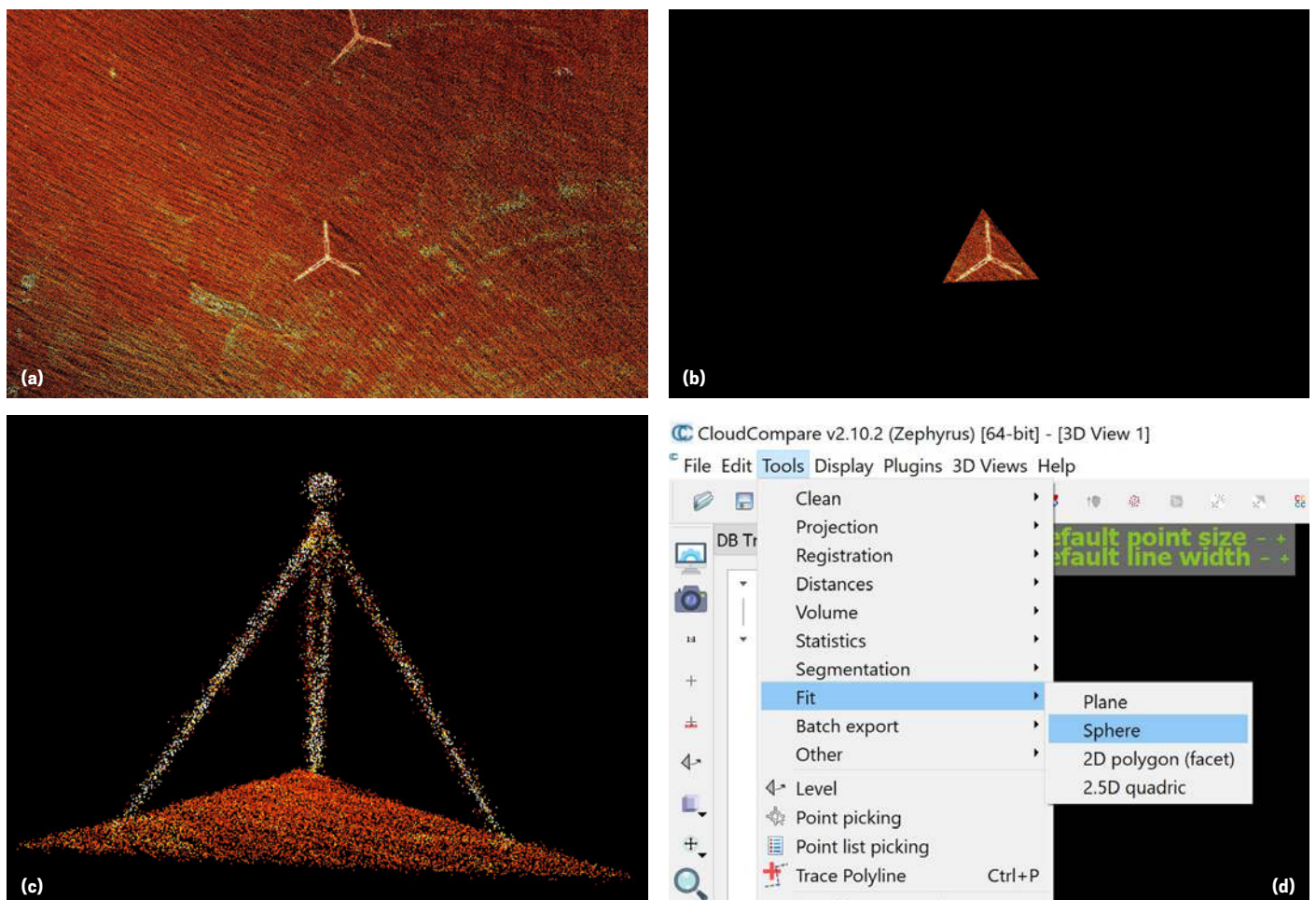


Figure 4 Creation of a ‘best-fit’ sphere in CloudCompare through (a-c) segmentation of the target sphere and the (d) Fit/Sphere function under the Tools menu.

This produced a new, virtual, sphere within the point cloud (Figure 5a) and corresponding entity within in the DB Tree window including a measure of the best-fit sphere radius (Figure 5b). This process was repeated for each of the spherical targets imaged within the scan and with the position of the sphere center recorded in a separate text file (e.g. *.csv) using Microsoft Excel.

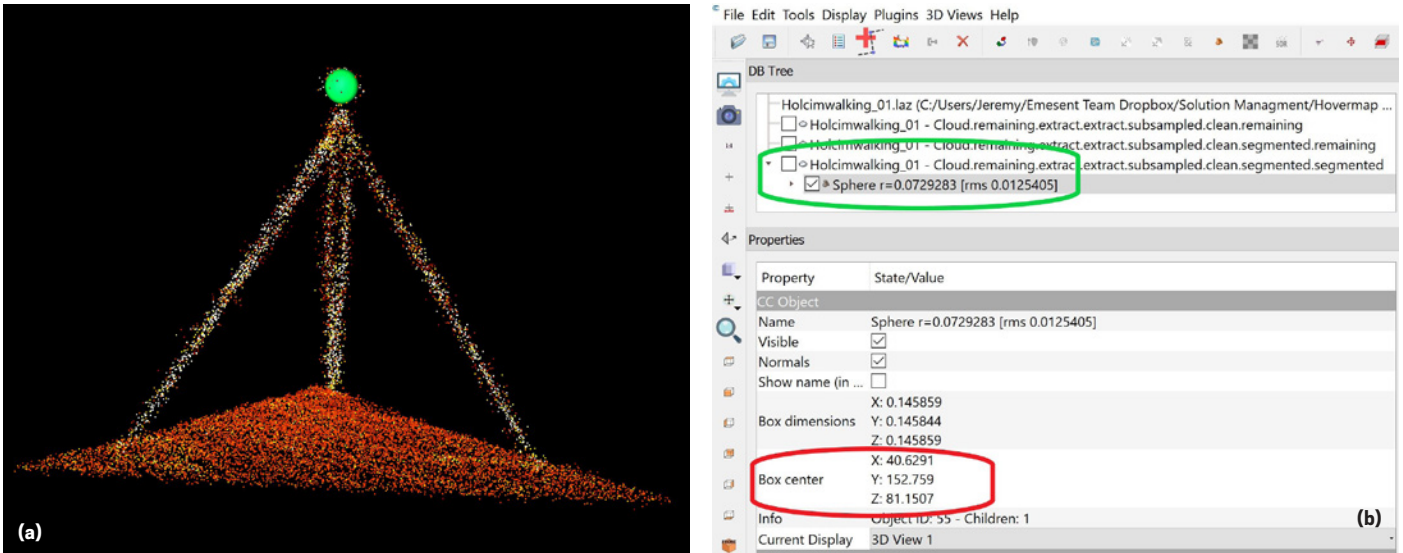


Figure 5 (a) 'Best-fit' Sphere created in CloudCompare and (b) showing the selection of the sphere entity (green) within the DB Tree to reveal the estimated sphere center (red) within the Properties window.

POINT CLOUD TO CONTROL ALIGNMENT

Registering the point cloud to control was achieved using the sphere centers and the Align tool within CloudCompare. In this, the saved sphere center data was imported and each paired with its corresponding control point ensuring that they were selected in identical order to avoid misalignment (Figure 6).

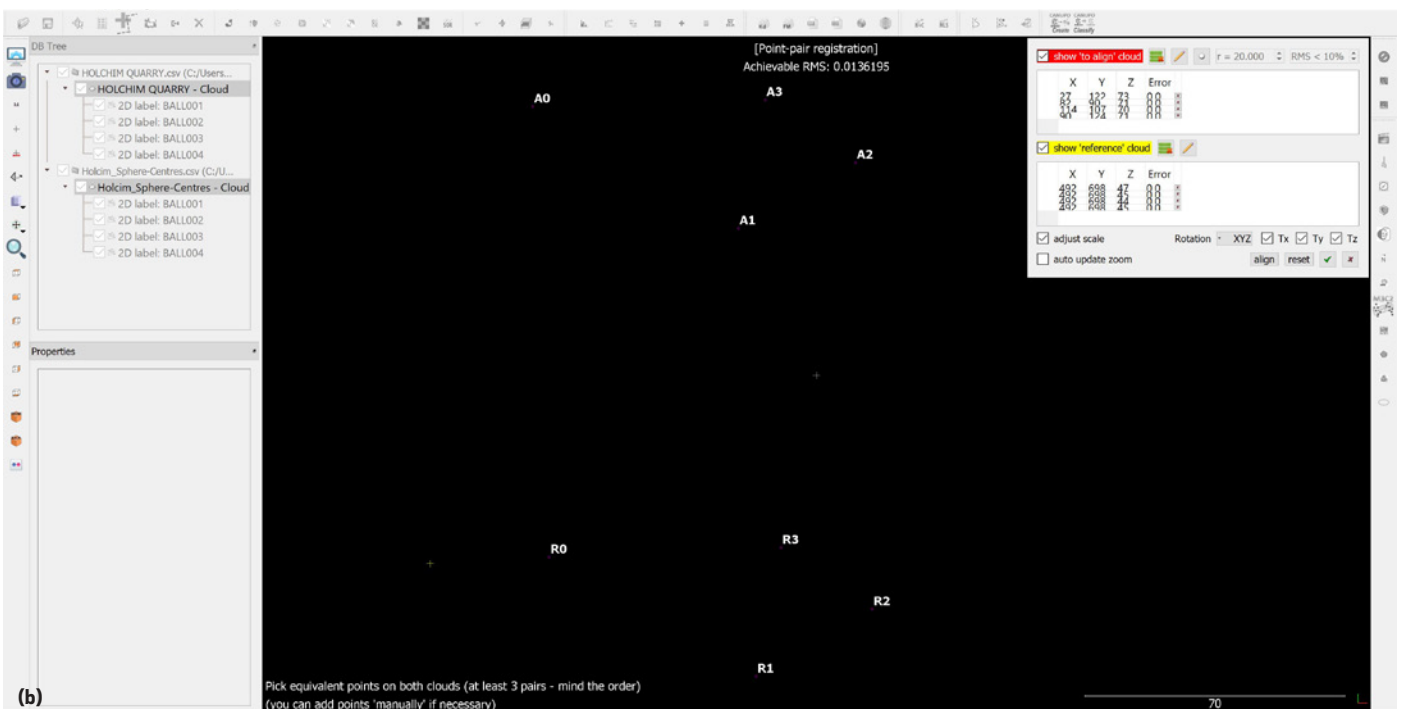


Figure 6 Picking corresponding points between the Reference (control) and sphere center (Hovermap) data using the Align tool.

The final transformation matrix from this alignment was saved as an ASCII file, with the final RMSE calculated at 0.014m (Figure 7).

The Hovermap point cloud was then unified into a single model and the transformation matrix of the sphere centers applied. The success of this alignment was qualitatively evaluated by viewing the point cloud spheres relative to the survey control (Figure 8).

A quantitative assessment was then achieved by computing the 3D distances between the geographic coordinates of both the control and sphere centers (Equation 1).

Equation 1

$$3D \text{ Distance} = \sqrt{(x_2 - x_1)^2 + (y_2 - y_1)^2 + (z_2 - z_1)^2}$$

Align info

Final RMS: 0.0136195

Transformation matrix

0.999	-0.013	-0.003	6.301
0.013	0.999	-0.001	-121.147
0.003	0.001	0.999	-26.414
0.000	0.000	0.000	1.000

Scale: 0.998936 (already integrated in above matrix!)

Refer to Console (F8) for more details

Figure 7 The final RMSE and transformation matrix following confirmation of the alignment.

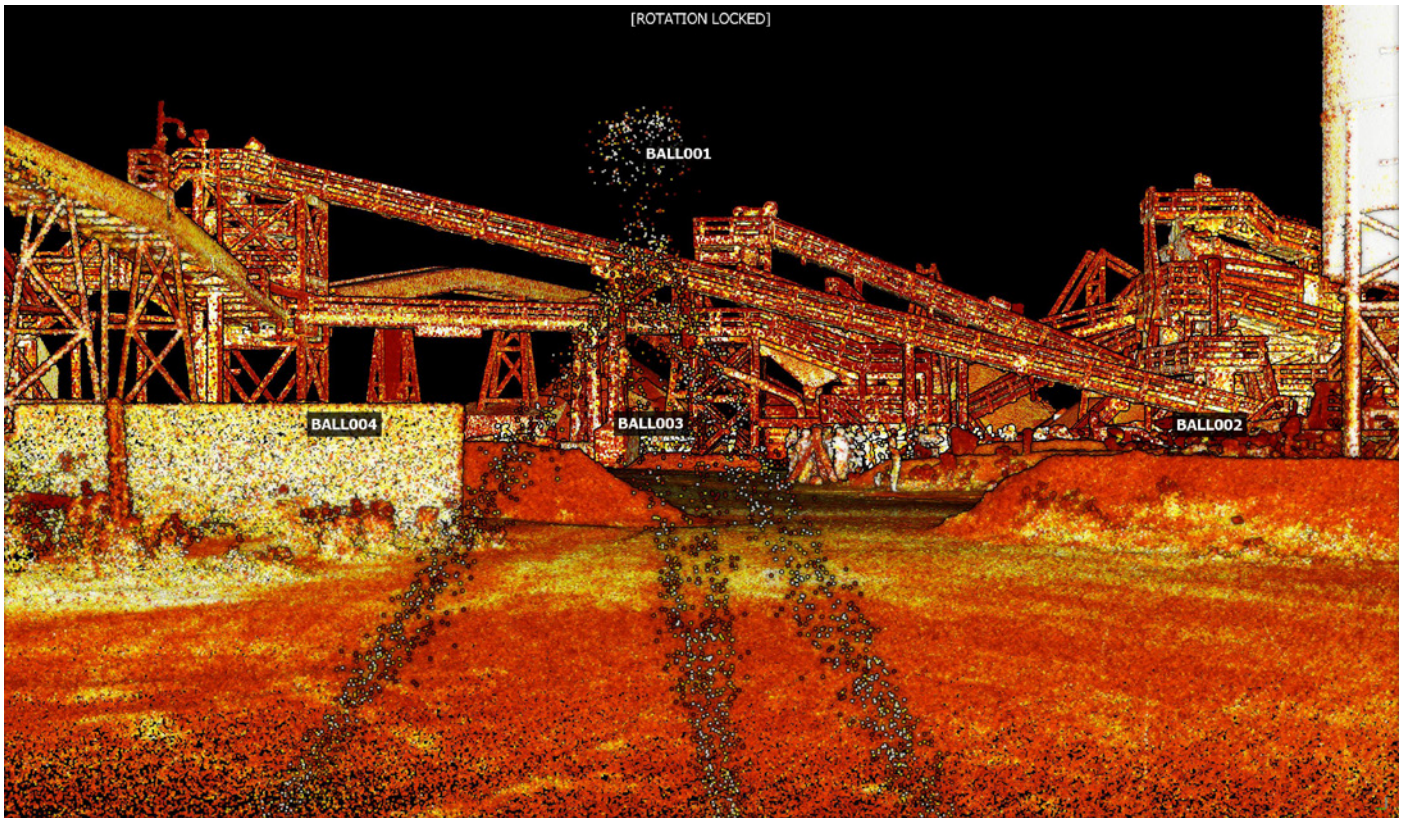


Figure 8 Visual check of the point cloud transformation to control.

RESULTS

In this study, utilizing the methods described above, we observed an initial RMSE of 0.014m (Figure 7) and with further interrogation, determined the geographic position of each sphere center (Table 2). This workflow also facilitated a point-for-point distance comparison with a mean 3D deviation of 0.013 ± 0.004 m (Table 3).

Two of the four targets, BALL03 and BALL04, reported the greatest 3D distances between the estimated sphere centers and control while also exhibiting the highest deviation between the estimated and true (~ 0.150 m \emptyset) sphere sizes. Evidence from examining the point cloud indicated that these two targets were not scanned as completely

(i.e. from all sides) as BALL01 and BALL02, and as a result, the best-fit sphere and corresponding centers were not as accurate. This highlights the importance of obtaining high-resolution data comprehensively on each target to achieve the optimal best-fit sphere and subsequent registration.

Given that the “typical” accuracy for a Velodyne VLP-16 sensor (currently utilized by Hovermap), as specified by Velodyne, is ± 0.030 m these results illustrate that Hovermap scanning is not only robust but, with the proprietary Emesent algorithms, also greater than the sum of its parts.

Table 2 Geographic coordinates of the control points and those of the ‘best-fit’ sphere centers as determined with the methods described in this report

GROUND CONTROL POINTS				BEST-FIT SPHERE CENTERS		
Target ID	Easting (X)	Northing (Y)	Elevation (Z)	Easting (X)	Northing (Y)	Elevation (Z)
BALL01	492732.010	6986501.751	47.098	492732.007	6986501.749	47.106
BALL02	492787.728	6986469.769	45.413	492787.729	6986469.775	45.405
BALL03	492818.940	6986487.831	44.949	492818.938	6986487.827	44.966
BALL04	492794.434	6986504.297	45.458	492794.439	6986504.297	45.442

Table 3 Details on the ‘best-fit’ diameter (\emptyset) of 0.015m spherical targets in CloudCompare and associated 1D and 3D distances between the survey control and the computed sphere centers

Target ID	Best-Fit Sphere \emptyset (m)	1D Distance (m)			3D Distance (m)
		Easting (X)	Northing (Y)	Elevation	X, Y, Z
BALL01	0.147	0.003	0.002	0.008	0.008
BALL02	0.148	0.001	0.006	0.008	0.010
BALL03	0.144	0.002	0.004	0.017	0.017
BALL04	0.142	0.005	<0.001	0.016	0.016
Mean \pm SD	0.145 ± 0.003	0.003 ± 0.001	0.003 ± 0.002	0.012 ± 0.005	0.013 ± 0.004

CONCLUSION

This evaluation of Hovermap accuracy used four laser scanning spheres as control points at a working quarry and calculated a ‘best-fit’ registration using the CloudCompare software package. The results shown here indicate that using a best-fit sphere registration method is appropriate when working with Hovermap data.

The Hovermap data in this study fitted the survey control with an RMSE of 14mm and achieved pair-wise 3D distances measurements with a mean deviation of 13mm \pm 4mm from ground truth.

These results also confirm that Emesent’s proprietary simultaneous localization and mapping (SLAM) algorithms enable Hovermap to achieve a level of accuracy that (a) meets survey requirements and (b) exceeds other mapping systems using the Velodyne VLP-16 sensor.



www.emesent.io

Copyright © 2020 Emesent. All rights reserved.
Version 1